



## A two-step nitrification model of ammonia and nitrite oxidation under benzene inhibitory and toxic effects in nitrifying batch cultures

Chérif Ben-Youssef<sup>a,b,\*</sup>, Alejandro Zepeda<sup>a</sup>, Anne-Claire Texier<sup>c</sup>, Jorge Gomez<sup>c</sup>

<sup>a</sup> Universidad Politécnica de Pachuca, Departamento de Biotecnología, Carr. Pachuca-Cd. Sahagún, km 20, Zempoala, 43084 Pachuca, Hgo., Mexico

<sup>b</sup> Instituto Tecnológico de Cancún, Av. Kabah km 3, 77500 Cancún, Q. Roo, Mexico

<sup>c</sup> Universidad Autónoma Metropolitana-Iztapalapa, Div. CBS, Departamento de Biotecnología, Av. San Rafael Atlixco 186, 09340 México, D.F., Mexico

### ARTICLE INFO

#### Article history:

Received 9 December 2008

Received in revised form 30 April 2009

Accepted 14 May 2009

#### Keywords:

Nitrifying sludge

Nitrification

Kinetic modeling

Benzene inhibition and toxicity

### ABSTRACT

The effect of benzene addition on the nitrifying activity of a sludge produced in steady-state nitrification was evaluated and modeled in batch cultures. The kinetic model was based on the sequential oxidation of ammonia to nitrite and nitrite to nitrate by two distinct bacterial groups. By taking separately benzene inhibitory and toxic effects explicitly into account, the proposed model was able to perform a reliable prediction of ammonia oxidation, nitrite oxidation, nitrate accumulation and benzene transformation with one set of kinetic parameters. The two-step nitrification model was validated using experimental data obtained from nitrifying batch cultures with variable initial concentrations of benzene (0, 7, 10 and 20 mg benzene-CI<sup>-1</sup>) and from additional batch cultures designed to evaluate specifically the toxic effect of cell preexposure to benzene concentrations (from 0 to 50 mg CI<sup>-1</sup>). In order to investigate the quality of the parameter estimates, standard deviation and correlation between parameters are provided via the Fisher Information Matrix, which full rank allowed establishing practical identifiability of the proposed model.

© 2009 Elsevier B.V. All rights reserved.

### 1. Introduction

Nitrification followed by denitrification is a widely used process for biological removal of nitrogen from wastewaters. Nitrification is in essence a two-step process involving the sequential oxidation of ammonia (NH<sub>4</sub><sup>+</sup>-N) to nitrite (NO<sub>2</sub><sup>-</sup>-N) and then to nitrate (NO<sub>3</sub><sup>-</sup>-N) by two distinct groups of oxidizing bacteria: the ammonia oxidizers and the nitrite oxidizers. The nitrification products can later be reduced to N<sub>2</sub> by heterotrophic or lithotrophic denitrifying bacteria in an anoxic environment. Nitrification processes have been traditionally described as one composite physiological process using single-step nitrification models that assume ammonia to nitrite oxidation to be the sole rate-limiting step throughout the oxidation sequence. However, in some cases, e.g. when nitrite oxidation becomes limiting, single-step models have been shown to erroneously describe batch ammonia oxidation profiles [1]. The use of two-step nitrification models has already been accurately investigated [2–6] and their implementation is especially essential when nitrite accumulation becomes important as a target product or an unwanted limiting intermediate.

The nitrifying bacteria are sensitive to a number of environmental factors, such as substrate concentration, pH, temperature, oxygen concentration and the presence of organic compounds. A large number of organic compounds can inhibit nitrification [7]. Benzene, toluene, ethylbenzene, and *o*-, *m*-, and *p*-xylene (BTEX) compounds have been found as contaminants in soils, sediments, and groundwater and have been classified as priority pollutants by the U.S. Environmental Protection Agency [8]. The BTEX compounds can adversely affect the efficiency of biological treatment systems because of their toxicity and recalcitrance to many microorganisms. Biodegradation of BTEX compounds by heterotrophic bacteria under anaerobic and aerobic conditions has already been explored [9,10]. However, very little attention has been paid to the toxicological or inhibitory influence of these compounds on lithoautotrophic nitrifying microorganisms [11–13].

The aim of this study was to propose a kinetic model able to predict the effect of different initial concentrations of benzene on a nitrifying sludge produced in steady-state nitrification in batch cultures. A two-step model expressed in terms of nitrogen species, i.e. the ammonium-oxidizing biomass and the nitrite-oxidizing biomass, which incorporates the inhibitory and toxic effects of benzene on the nitrification kinetics, is proposed. The model is then validated on the basis of the experimental concentrations of ammonia, nitrite, nitrate and benzene obtained during four batch cultures corresponding to initial concentration of 0, 7, 10 and 20 mg benzene-CI<sup>-1</sup>. Finding the best-fit parameters is not the end of

\* Corresponding author at: Instituto Tecnológico de Cancún, Av. Kabah km 3, 77500 Cancún, Q. Roo, Mexico. Tel.: +52 998 8807432x115; fax: +52 998 8807433.

E-mail address: [cherifby@itcancun.edu.mx](mailto:cherifby@itcancun.edu.mx) (C. Ben-Youssef).

parameter estimation. In order for the parameter values to be meaningful, they need to be accompanied by an estimation of their quality. This was done by a sensitivity analysis and the approximation of standard deviations for the estimated parameters using the Fisher Information Matrix (FIM), which also allowed establishing practical identifiability and estimating the correlation between parameters.

## 2. Materials and methods

### 2.1. Nitrifying sludge

The sludge used for inoculating batch reactors was obtained from a continuous stirred nitrifying 3-l reactor. The system was kept operating continuously for over 2 years under steady-state nitrification at 300 rpm, 30 °C, pH value of  $8.0 \pm 0.5$ , a constant airflow of two volumes of air per volume of liquid per minute and a hydraulic retention time of 2.2 days. Steady-state operating conditions and performance of the continuous reactor have been described previously in [13].

### 2.2. Batch cultures

A detailed description of the batch culture medium composition and batch operating conditions is reported in [13]. In brief, all batch experiments were performed in 120 ml serologic bottles with a working volume of 50 ml with an initial microbial protein concentration of  $150 \pm 10 \text{ mg l}^{-1}$ . The initial  $\text{NH}_4^+\text{-N}$  concentration was  $100 \pm 10 \text{ mg l}^{-1}$ . The cultures were placed on an orbital shaker working at 200 rpm at 30 °C for 16 h. Initial pH value was  $8.5 \pm 0.5$  in all cases. For nitrification and benzene removal kinetic study, cultures were incubated in the presence of benzene at 0, 7, 10, and 20 mg benzene- $\text{Cl}^{-1}$  and samples were withdrawn at different times over a period of 100 h, filtered ( $0.45 \mu\text{m}$ ) and analyzed for ammonia, nitrite, nitrate and benzene. All batch cultures were carried out at least in duplicate. Possible loss of benzene due to volatilization and adsorption on bacterial sludge was monitored by using abiotic and sterile controls.

### 2.3. Analytical methods

Headspace and liquid concentrations of benzene in the bottles were analyzed by gas chromatography (Varian Star Model 3400) using a flame ionization detector. Ammonium nitrogen ( $\text{NH}_4^+\text{-N}$ ) was analyzed by a selective electrode (Phoenix Electrode Co., USA). Nitrite and nitrate were analyzed by capillary electrophoresis (Waters Capillary Ion Analyzer). Lowry's method was employed to measure microbial protein concentration. All experimental conditions used for the analytical methods formerly mentioned were previously described in [13]. Analytical methods had a variation coefficient of less than 10%.

## 3. Model development

### 3.1. A two-step nitrification with benzene transformation

Benzene addition in the nitrifying cultures used in this study has been shown not only to inhibit the consumption rate of  $\text{NH}_4^+\text{-N}$ , but also to affect in a different way the oxidation of  $\text{NO}_2^-\text{-N}$  and consequently the production rate of  $\text{NO}_3^-\text{-N}$  [12,13]. To quantify and predict the benzene effects on the ammonium, nitrite and nitrate kinetics separately, it appeared necessary to consider a two-step nitrification model structure based on the individual characterization of both ammonia and nitrite oxidation. Modeling the two-step process involves the use of two state variables corresponding to the

concentration of ammonium-oxidizing biomass ( $X_A$ ) and the concentration of nitrite-oxidizing biomass ( $X_N$ ). In the first nitrification step, ammonia is oxidized by the  $X_A$  bacteria, which produce nitrite and grow. In the second step, nitrite is oxidized by the  $X_N$  microbial population through a reaction yielding to nitrate production and its own growth.

Since results from [12,13] showed that benzene addition in batch cultures caused clear inhibitory and toxic effects on ammonia and nitrite oxidation reactions, and since benzene concentration was monitored during the experiments, a dynamical equation describing benzene transformation is incorporated to complete the two-step model. Furthermore, the following assumptions are made to reduce the complexity of the kinetic model:

- (1) Dissolved oxygen uptake is not considered in the reaction kinetics since no limitation for oxygen was observed in the batch cultures [13]. In particular, it was verified that the dissolved oxygen concentration dropped to  $5.3 \pm 0.2 \text{ mg l}^{-1}$  after 16 h.
- (2) During all the experiments, the yield for biomass formation was  $0.011 \pm 0.003 \text{ g microbial protein-N/g consumed NH}_4^+\text{-N}$  and biomass concentration did not change significantly (from an initial concentration of  $150 \pm 10 \text{ mg l}^{-1}$  to a final concentration of  $155 \pm 10 \text{ mg l}^{-1}$ ), i.e. the process was mainly deassimilative [13]. Hence, as expected in short-term low-loaded batch cultures, growth and decay are neglected in the model.
- (3) Benzene transformation is assumed to be carried out by the AMO enzyme [12–16]. It was then assumed that benzene degradation was done by  $X_A$ .

Under assumptions (1)–(3), the following set of first-order differential equations describes ammonium oxidation, nitrite oxidation, nitrate accumulation and benzene transformation:

$$\frac{dS_{\text{NH}_4}}{dt} = -q_{\text{NH}_4} X_A \quad (1)$$

$$\frac{dS_{\text{NO}_2}}{dt} = Y_{\text{PA}} q_{\text{NH}_4} X_A - q_{\text{NO}_2} X_N \quad (2)$$

$$\frac{dS_{\text{NO}_3}}{dt} = Y_{\text{PN}} q_{\text{NO}_2} X_N \quad (3)$$

$$\frac{dS_{\text{BZ}}}{dt} = -q_{\text{BZ,A}} X_A \quad (4)$$

where  $S_{\text{NH}_4}$ ,  $S_{\text{NO}_2}$ ,  $S_{\text{NO}_3}$  and  $S_{\text{BZ}}$  represent the concentration of ammonium, nitrite, nitrate and benzene, respectively.  $q_{\text{NH}_4}$  is the specific rate of ammonium oxidation,  $q_{\text{NO}_2}$  the specific rate of nitrite oxidation and  $q_{\text{BZ,A}}$  the specific rate of benzene transformation.  $Y_{\text{PA}}$  is the yield coefficient for nitrite from ammonium and  $Y_{\text{PN}}$  is the yield coefficient for nitrate from nitrite.

At this stage, it has to be emphasized that initial values of  $X_A$  and  $X_N$  are necessary to implement the model dynamics. The task of experimental determination of  $X_A$  and  $X_N$  concentrations or, even more specifically, their respective active fraction, is generally not trivial in nitrification processes. This is particularly the case considering the heterogeneity of the nitrifying microbial consortium under study. An alternative to the unavailability of  $X_A$  and  $X_N$  measurements is to estimate them as fractions of the total biomass concentration according to stoichiometric considerations [1,5] or to consider the nitrification kinetics in terms of volumetric rather than specific oxidation rates. In this work, the volumetric rate of ammonium oxidation  $r_{\text{NH}_4} = q_{\text{NH}_4} X_A$ , of nitrite oxidation  $r_{\text{NO}_2} = q_{\text{NO}_2} X_N$  and benzene transformation  $r_{\text{BZ,A}} = q_{\text{BZ,A}} X_A$  was introduced.

### 3.2. Inhibition effect of benzene

Because of the two-step nitrification reaction scheme adopted in this work, benzene inhibition effect on ammonia oxidizers and

nitrite oxidizers activity has to be considered separately. In this study, noncompetitive inhibition is considered and the related mechanisms are mathematically modeled by adding a common hyperbolic inhibition term to the Monod expression, yielding to the following expressions for the volumetric oxidation rate of ammonium ( $r_{\text{NH}_4}$ ) and nitrite ( $r_{\text{NO}_2}$ ):

$$r_{\text{NH}_4} = \bar{r}_{\text{max,NH}_4} \frac{S_{\text{NH}_4}}{K_{\text{S,A}} + S_{\text{NH}_4}} \cdot \frac{K_{i,A}}{K_{i,A} + S_{\text{BZ}}} \quad (5)$$

$$r_{\text{NO}_2} = \bar{r}_{\text{max,NO}_2} \frac{S_{\text{NO}_2}}{K_{\text{S,N}} + S_{\text{NO}_2}} \cdot \frac{K_{i,N}}{K_{i,N} + S_{\text{BZ}}} \quad (6)$$

where  $\bar{r}_{\text{max,NH}_4}$  and  $\bar{r}_{\text{max,NO}_2}$  correspond to the maximum volumetric oxidation rates,  $K_{\text{S,A}}$  and  $K_{\text{S,N}}$  are affinity constants and  $K_{i,A}$  and  $K_{i,N}$  are benzene inhibition constants on the  $X_A$  and  $X_B$  oxidation activity, respectively.

The volumetric transformation rate of benzene to metabolic intermediates was modeled according to a Yano and Koga's model [17]:

$$r_{\text{BZ,A}} = r_{\text{max,BZ}} \frac{S_{\text{BZ}}}{K_{\text{S,BZ}} + S_{\text{BZ}} + S_{\text{BZ}}^3/K_{i,\text{BZ}}} \quad (7)$$

where  $r_{\text{max,BZ}}$  is the maximum transformation rate of benzene,  $K_{\text{S,BZ}}$  is the affinity constant of  $X_A$  for benzene and  $K_{i,\text{BZ}}$  the inhibition constant for benzene consumption. Eq. (7) has been selected after testing various model structures of benzene inhibition on benzene transformation rate, in particular the classic Haldane equation. However, simulation tests have shown that a conventional Haldane model was insufficient to predict high benzene inhibition levels on  $r_{\text{BZ,A}}$ , in particular for those experiments with initial benzene concentrations  $S_{\text{BZ}}(0) \geq 20 \text{ mg C l}^{-1}$ .

### 3.3. Toxic effect of benzene

At this stage, the nitrification model given by Eqs. (1)–(7) may be used to predict benzene inhibition on the nitrifying activity. However, in [13], additional experimental tests in batch cultures were carried out in order to evaluate the toxicity of benzene on the nitrifying sludge. These tests consisted in 16 h batch cultures at different benzene initial concentrations ( $S_{\text{BZ}}(0) = 0\text{--}50 \text{ mg C l}^{-1}$ ), washing the pellets from each batch culture with a solution of NaCl ( $9 \text{ g l}^{-1}$ ) and reusing the same inoculum in 16 h nitrifying batch cultures without benzene. Results indicated that exposure of cells to benzene concentrations of  $20\text{--}50 \text{ mg C l}^{-1}$  caused a decrease not only on the consumption efficiency of ammonium by  $X_A$  but also on the nitrite conversion into nitrate by  $X_B$ . From the modeling viewpoint, typical mathematical expression accounting for inhibition, such as hyperbolic or Haldane types, are not able to predict such a mechanism since without benzene in the cultures, the oxidation rates are reduced to simple substrate-limiting expressions, i.e. Eqs. (5) and (6) correspond to Monod equations when  $S_{\text{BZ}} = 0$ . Some authors have suggested that this kind of negative effect is probably due to the harmful effect of hydrocarbons on the functioning of biological membranes [18–23]. In the absence of specific experiments, the fact that bacteria did not totally recover their nitrifying activity after previous exposure to benzene may be interpreted as a consequence of different factors, e.g. loss of viability, increased adaptation times to initiate nitrification and/or decrease in the ammonia and nitrite oxidation activity. In this study, it was only considered a reduction of the nitrification oxidation rates due to preexposure to benzene. From the modeling viewpoint, this may be done by modulating the volumetric consumption rate of ammonium in Eq. (5) and nitrite in Eq. (6) as a function of the initial benzene concentration the cells

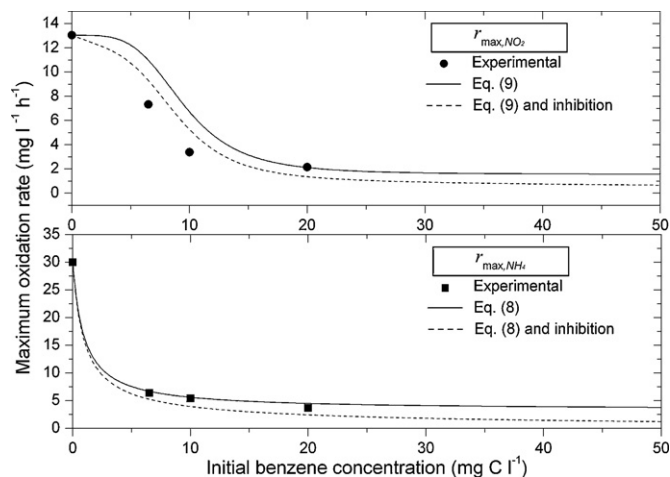


Fig. 1. Maximum volumetric rate of ammonium oxidation (line) and nitrite oxidation (dashed line) after preexposure to different initial benzene concentrations. Experimental data (symbols) and model predicted (lines).

were previously exposed to, as follows:

$$\bar{r}_{\text{max,NH}_4} = r_{\text{max,NH}_4} \left( \delta_A + \frac{1 - \delta_A}{1 + S_{\text{BZ}}^p(0)/K_{t,A}} \right) \quad (8)$$

$$\bar{r}_{\text{max,NO}_2} = r_{\text{max,NO}_2} \left( \delta_N + \frac{1 - \delta_N}{1 + (S_{\text{BZ}}^p(0)/K_{t,N})^4} \right) \quad (9)$$

where  $S_{\text{BZ}}^p(0)$  is the initial concentration of benzene during the preexposure,  $r_{\text{max,NH}_4}$  and  $r_{\text{max,NO}_2}$  correspond to the nominal maximum rate of ammonia and nitrite oxidation,  $\delta_A$  and  $\delta_N$  are constants representing the percentage of residual oxidation activity and  $K_{t,A}$  and  $K_{t,N}$  are benzene toxicity constants for  $X_A$  and  $X_N$ , respectively. Fig. 1 illustrates the evolution of the experimental and modeled maximum oxidation rate of ammonium (Eq. (8)) and nitrite (Eq. (9)) as a function of the initial benzene concentration using the kinetic parameter values given in Table 1. The choice of such functions was based on the fact that the toxicity experiments illustrated a sigmoid-type of evolution of the maximum volumetric oxidation rates from the nominal value at  $S_{\text{BZ}}^p(0) = 0 \text{ mg benzene-C l}^{-1}$  to a minimum final value at high benzene concentrations, i.e. at  $S_{\text{BZ}}^p(0) = 50 \text{ mg benzene-C l}^{-1}$ . This final minimum value was expressed as a percentage of the maximum volumetric oxidation rates by defining the  $\delta_A$  and  $\delta_N$  constants in Eqs. (8) and (9). In order to generate a more pronounced sigmoid shape for the nitrite maximum oxidation rate (see Fig. 1), the exponent in the denominator in Eq. (9) was increased and finally set to 4 after intensive simulations of the complete model, and good fitting results are observed between experimental data and model predictions.

### 3.4. Parameter estimation

There are several methods of parameter estimation for model calibration. A model may be fitted either via a numerical method, such as least squares or a quadratic estimation method, or via a heuristic method. In this study, the most commonly used approach for model calibration, which consists in minimizing a weighted sum of squared errors (see Eq. (10)) between model,  $y(t_k, \theta)$ , and measured outputs,  $y_m(t_k)$ , with the weights  $Q_k$  and  $N$  the number of measurements at times  $t_k$ , was implemented:

$$J(\theta) = \sum_{k=1}^N (y(t_k, \theta) - y_m(t_k))^T Q_k (y(t_k, \theta) - y_m(t_k)) \quad (10)$$

**Table 1**  
Kinetic parameters, standard errors (absolute and relative) and correlation matrix.

Parameter	Estimate	Standard error		Correlation matrix												
		Absolute	Relative	$Y_{PA}$	$K_{S,A}$	$K_{i,A}$	$K_{t,A}$	$\delta_A$	$Y_{PN}$	$K_{S,N}$	$K_{i,N}$	$K_{t,N}$	$\delta_N$	$K_{S,BZ}$	$K_{i,BZ}$	
$Y_{PA}$	0.91	0.08	0.09	1.00												
$K_{S,A}$	1.80	2.49	1.38	0.10	1.00											
$K_{i,A}$	23.80	4.58	0.19	0.00	0.02	1.00										
$K_{t,A}$	0.95	0.23	0.24	0.17	0.47	0.05	1.00									
$\delta_A$	0.11	0.02	0.14	-0.15	0.18	-0.56	-0.58	1.00								
$Y_{PN}$	1.00	0.11	0.11	-0.87	-0.11	0.00	-0.21	0.12	1.00							
$K_{S,N}$	1.90	1.51	0.79	-0.60	-0.08	-0.06	-0.07	0.03	0.60	1.00						
$K_{i,N}$	36.20	24.16	0.67	0.10	0.03	0.34	0.07	-0.23	-0.06	-0.22	1.00					
$K_{t,N}$	9.50	1.64	0.17	-0.27	-0.06	-0.15	0.03	0.00	0.25	0.71	-0.57	1.00				
$\delta_N$	0.12	0.03	0.25	0.43	0.04	-0.25	-0.07	0.23	-0.43	-0.26	-0.62	-0.08	1.00			
$K_{S,BZ}$	1.85	1.88	1.01	0.00	-0.03	-0.05	0.22	-0.13	-0.01	-0.01	-0.02	0.02	-0.02	1.00		
$K_{i,BZ}$	46.10	5.88	0.13	0.01	-0.01	-0.06	0.13	-0.08	-0.01	-0.01	-0.02	0.01	-0.01	0.71	1.00	
Parameter	Constant			Standard error						Reference						
				Absolute			Relative									
$r_{\max,NH_4}$		30.01 <sup>a</sup>		1.89			0.063							[13]		
$r_{\max,NO_2}$		13.04 <sup>a</sup>		0.72			0.055							[13]		
$r_{\max,BZ}$		0.816 <sup>a</sup>		0.072			0.088							[13]		

<sup>a</sup> These are the volumetric rate values used to calculate the specific rates values given in [13].

Notice that the weighting matrix  $Q_k$  in Eq. (10) is chosen as the inverse measurement error covariance matrix. The search for the best-fit parameters ( $\hat{\theta}$ ) of the nitrification model previously described would be tedious if all the 15 parameters had to be estimated. Moreover, from the identifiability point of view, not all the two-step oxidation related parameters could be reliably estimated using only short-time batch total biomass concentration profiles and specific experiments would be required. Here, the maximum volumetric oxidation rate of ammonia and nitrite, i.e.  $\bar{r}_{\max,NH_4}$  and  $\bar{r}_{\max,NO_2}$ , and the maximum volumetric transformation rate of benzene  $r_{\max,BZ}$  were fixed to their experimental value [13]. The resting parameters were estimated using the nonlinear least-square function *lsqnonlin* (with the Levenberg–Marquardt algorithm option) provided in the Optimization toolbox of MATLAB 7.2. To reduce the complexity of the parameter estimation procedure, the parameters were divided into two subsets, one corresponding to the benzene transformation parameters, and the other one to the ammonia and nitrite oxidations. The constant and estimated kinetic parameters values used for model simulation are listed in Table 1. Simulations were obtained by using the dynamical model given by Eqs. (1)–(9) and a fourth order Runge–Kutta algorithm for numerical integration of the ordinary differential equations. Measurement errors of 10% were assumed for all the variables of the nitrification process and elements of the matrix weights  $Q_k$  were set to zero for a concentration detection limit of 1 mg<sup>-1</sup>.

### 3.5. Parameter accuracy and practical identifiability

A study of the structural identifiability of model parameters prior to practical model application is a key task in modeling biokinetics [24]. This problem is difficult to solve here because of the high number of parameters to be estimated (12) and the complexity of the model. In turn, practical identifiability may be established by a useful test suggested by [25], which consists in checking the full rank of the Fisher Information Matrix. In this work, since the weighting matrix  $Q_k$  in Eq. (10) was chosen as the inverse measurement error covariance matrix, assuming that the measurement noise is white (i.e. independent and normally distributed with zero mean), and uncorrelated (i.e. the measurement error covariance matrix is a diagonal matrix), it was thus possible to approximate the estimated parameter estimation error covariance matrix  $V$  as

the inverse of the Fisher Information Matrix (FIM) [26,27]:

$$V = \text{FIM}^{-1} = \left[ \sum_{k=1}^N \left( \frac{\partial y(t_k)}{\partial \theta} \right)^T Q_k \left( \frac{\partial y(t_k)}{\partial \theta} \right) \right]^{-1} \quad (11)$$

The FIM expresses the information content of the experiments by combining the sensitivity functions  $\partial y/\partial \theta$  of the estimated parameter vector  $\theta$  with respect to the output measurable vector  $y$  and measurement accuracy. The more a measurement is noise corrupted the less it will count in the FIM. The standard deviation of the  $i$ th estimated parameter  $\theta_i$  ( $i = 1$  to  $p$ ),  $\sigma(\theta_i)$ , is calculated using  $V_{ii}$ , the  $i$ th diagonal element of the estimation error covariance matrix  $V$  (Eq. (11)), and the optimal value of the cost function  $J(\hat{\theta})$  (Eq. (10)) according to:

$$\sigma(\theta_i) = \sqrt{\frac{J(\hat{\theta})}{N-p}} \cdot V_{ii} \quad (12)$$

The sensitivity functions  $\partial y/\partial \theta$  of the estimated parameter vector used in Eq. (11) were calculated using the complex-step approximation method [28,29] which main advantage over the commonly used finite difference approach is that it does not involve a difference operation and is therefore not subjected to round-off errors or subtractive cancellation, even if extremely small parameter variation steps are used.

## 4. Results and discussion

### 4.1. Kinetic modeling

The experimental and model-predicted data of ammonia, nitrite, nitrate and benzene concentrations in batch cultures are illustrated in Fig. 2 for initial benzene concentrations  $S_{BZ}(0) = 0, 7, 10,$  and  $20 \text{ mg C l}^{-1}$ , respectively. The predicted values are seen to be in reasonable agreement with the experimental data for all the tested initial benzene concentrations, particularly if it is considered that the model depicts all the experimental profiles by using only a unique set of kinetic parameters. In addition, the root mean square error (RMSE) is used to measure the difference between the actual and model-predicted values of ammonia, nitrite, nitrate and benzene concentrations (see Table 2). It may be seen from these results that the RMSE is always less than 2 mg benzene-C l<sup>-1</sup> for benzene

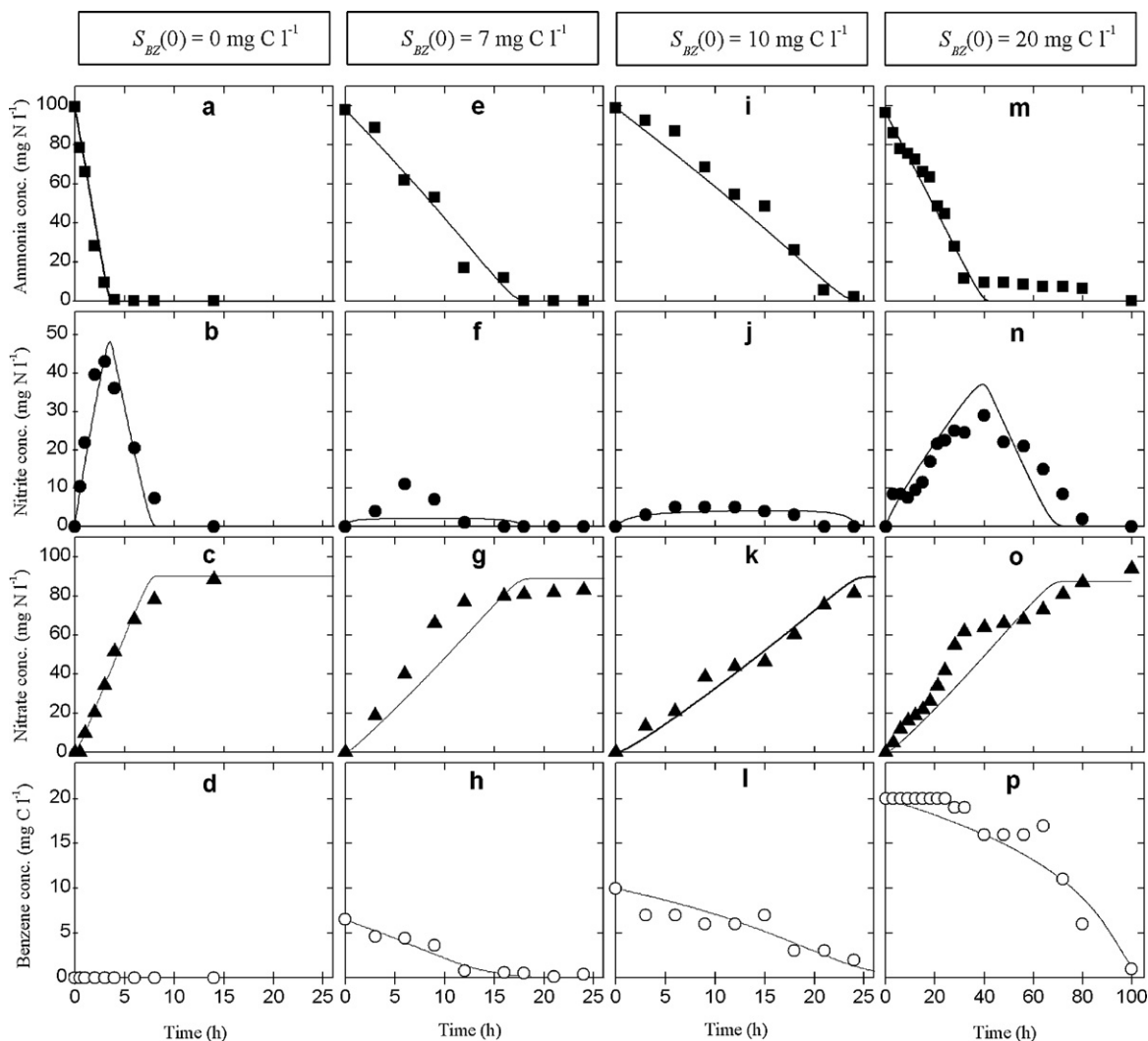


**Fig. 2.** Kinetic profiles of the measured (symbols) and predicted (lines) concentrations of ammonia (■), nitrite (●), nitrate (▲) and benzene (○). Experiment with initial benzene concentration  $S_{BZ}(0)$  (in  $\text{mg C l}^{-1}$ ) at 0 (a–d), 7 (e–h), 10 (i–l) and 20 (m–p).

and less than  $12.8 \text{ mg N l}^{-1}$  for ammonia, nitrite and nitrate, which are acceptable values when compared to the 10% maximum variation coefficient of the analytical methods. The benzene inhibition effect on ammonia oxidation, which basically consisted in larger consumption time of ammonia, i.e. from 5 h for the control experiment (Fig. 2a–d) up to 80 h for the experiment carried out with the highest benzene concentration (Fig. 2m–p), was adequately predicted by the proposed model. Similar observations may be made with respect to the nitrate formation profiles. When considering increasing concentrations of benzene, the nitrite concentration profiles are following a different pattern, i.e. reaching first a maximum nitrite accumulation of  $43 \pm 4 \text{ mg N l}^{-1}$  without the presence of benzene in the medium, subsequent lower maximum concentrations  $S_{\text{NO}_2} \leq 10 \text{ mg N l}^{-1}$  for  $S_{BZ}(0) = 7\text{--}10 \text{ mg benzene-C l}^{-1}$  and, finally, increased nitrite accumulation of  $28 \pm 2 \text{ mg N l}^{-1}$  for the highest benzene concentration of  $S_{BZ}(0) = 20 \text{ mg benzene-C l}^{-1}$ , and

yet, the predicted values fit this general tendency with a maximum absolute error of  $5 \text{ mg N l}^{-1}$  for some experimental points.

The results of the additional batch cultures for evaluating the toxicity of benzene on the nitrifying bacteria are illustrated in Fig. 3. This figure shows the evolution of measured and model-predicted final concentrations of ammonia, nitrite and nitrate as a function of initial benzene concentrations (from 0 up to  $50 \text{ mg benzene-C l}^{-1}$ ) when the microbial sludge was exposed during 16 h to benzene (Fig. 3a) and then washed and reused in nitrifying 16 h batch cultures without benzene (Fig. 3b). Notice that the X-axis of Fig. 3b shows the initial benzene concentration the cells were pre-exposed to during the first batch cultures, i.e.  $S_{BZ}^p(0)$ , understanding that no benzene is present during these experiments. Adequate fitting between experimental data and model predictions is obtained using the same set of kinetic parameter values given in Table 1. The RMSE of the corresponding experiments are given in the last two

**Table 2**  
Absolute and relative (in parenthesis) root mean square error (RMSE) between experimental and model-predicted data.

Experiment	$S_{BZ}(0) = 0 \text{ mg C l}^{-1}$	$S_{BZ}(0) = 7 \text{ mg C l}^{-1}$	$S_{BZ}(0) = 10 \text{ mg C l}^{-1}$	$S_{BZ}(0) = 20 \text{ mg C l}^{-1}$	Experiment Fig. 3a	Experiment Fig. 3b
$S_{\text{NH}_4}$	5.05 (0.14)	5.67 (0.26)	6.47 (0.20)	6.18 (0.11)	9.50 (0.21)	8.58 (0.26)
$S_{\text{NO}_2}$	4.82 (0.16)	3.55 (1.71)	1.53 (0.39)	5.10 (0.49)	6.77 (0.53)	2.65 (0.05)
$S_{\text{NO}_3}$	4.66 (0.33)	11.50 (0.31)	5.16 (0.28)	10.51 (0.58)	10.70 (1.09)	6.71 (0.26)
$S_{BZ}$	–	0.51 (0.13)	1.24 (0.19)	1.77 (0.13)	–	–

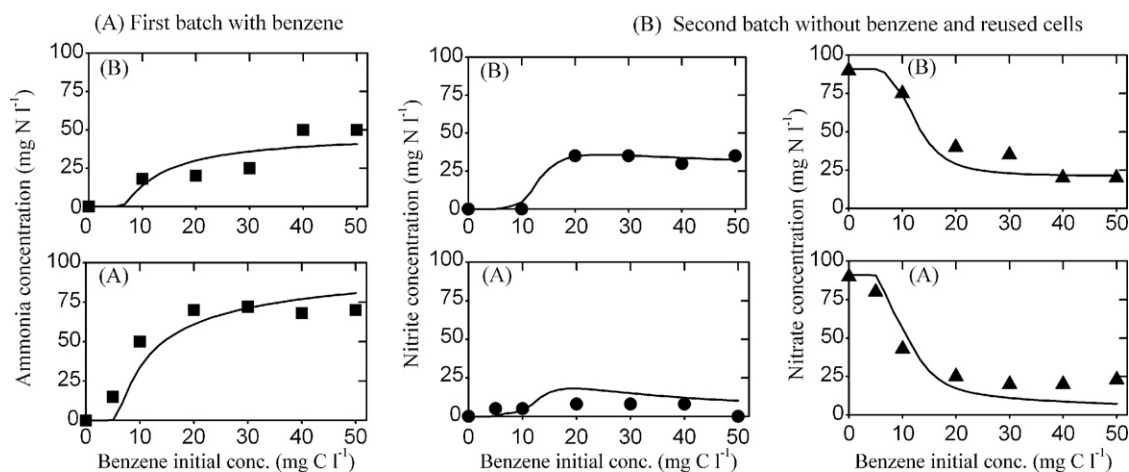


**Fig. 3.** Measured (symbols) and predicted (lines) concentrations of ammonia (■), nitrite (●) and nitrate (▲) as a function of initial benzene concentration. Each point was determined after 16 h batch cultures at different benzene initial concentrations (a) and when the inoculum was reused in 16 h batch cultures without benzene (b).

columns of Table 2. The RMSE errors obtained for the experiment corresponding to the second batch without benzene are smaller, i.e. less than  $8.93 \text{ mg N l}^{-1}$  for the nitrogenous compounds, than the values obtained for the first batch with benzene, i.e. less than  $14.46 \text{ mg N l}^{-1}$ . This may be explained by the fact that the proposed model is based on an instantaneous benzene toxic effect on the two oxidation steps, i.e. a toxic effect that takes place immediately at  $t=0$  according to Eqs. (8) and (9). Toxic effect of the preexposure of the nitrifying sludge to benzene is clearly observed, in particular for initial concentrations  $S_{\text{BZ}}^{\text{p}}(0) \geq 10 \text{ mg benzene-C l}^{-1}$  for ammonia consumption process and  $S_{\text{BZ}}^{\text{p}}(0) \geq 20 \text{ mg benzene-C l}^{-1}$  for nitrite oxidation process. This is in accordance with the results that would have been expected when using the mathematical expressions of maximum oxidation rates given by Eqs. (8) and (9). The numerical simulation of these equations illustrates how the benzene toxic effect is more important on the ammonia-oxidizing activity. Indeed, as shown in Fig. 1, the maximum volumetric ammonium oxidation rate decreases rapidly as soon as benzene is present in the medium, while the maximum volumetric nitrite oxidation rate decreases significantly only after  $S_{\text{BZ}}^{\text{p}}(0) \geq 10 \text{ mg C l}^{-1}$ . Fig. 1 depicts how ammonium and nitrite maximum oxidation rates  $\bar{r}_{\text{max, NH}_4}$  and  $\bar{r}_{\text{max, NO}_2}$  are tending towards their respective residual activity level ( $\delta_A$  and  $\delta_N$  are 11% and 12%, respectively, according to the proposed model) as benzene concentration is increasing. The experimental data (Fig. 3b) also confirm this model feature, in particular when observing the stabilization tendency of nitrite oxidation at  $S_{\text{BZ}}^{\text{p}}(0) \geq 30 \text{ mg C l}^{-1}$ . In order to establish practical identifiability and to obtain approximate standard deviations for the estimated parameters, the parameter estimation error covariance matrix  $V$  was calculated using Eq. (11). The FIM was first checked to be full rank, i.e.  $\text{rank}(\text{FIM}) = 12$ , which established practical identifiability. The sensitivity functions  $\partial y / \partial \theta$  in Eq. (11) were calculated for all the data points using an imaginary step  $\Delta\theta = 1e^{-20}$ . The standard deviations values (absolute and relative) of the estimated parameters were then obtained using Eq. (12) and are listed in Table 1 together with the corresponding correlation matrix. From these results, we may observe that the most accurate parameters correspond to the yield constants  $Y_{\text{PA}}$  and  $Y_{\text{PN}}$  with a relative standard error of 9% and 11%, respectively. Most of the remaining standard deviations are of relatively acceptable accuracy considering the 10% measurement inaccuracy except for the affinity constants  $K_{\text{S,A}}$  and  $K_{\text{S,BZ}}$ , which present standard deviations of 138% and 101%, respectively. The occurrence indicates that the experimental setup was insufficient to allow these parameter values to be accurately estimated, resulting in poor parameter identifiability. Actually, Optimal Experimental

Design (OED) for parameter estimation should be performed to improve the quality of the experimental data for improved parameter identification. From the correlation matrix (Table 1), we may observe that the most correlated parameters are the yield constants  $Y_{\text{PA}}$  and  $Y_{\text{PN}}$  with a covariance value of 0.87. Although this may indicate poor parameter identifiability, the corresponding standard errors are, as described earlier, of good quality, which permits a certain confidence on these estimated values. On the other hand, parameters related to benzene dynamics, i.e.  $K_{\text{S,BZ}}$  and  $K_{\text{i,BZ}}$  present an important correlation coefficient of 0.71 associated with an important standard error in the case of the affinity constant  $K_{\text{S,BZ}}$ , indicating that the value of this last parameter should be taken with great care due to its poor parameter identifiability. OED is also specially recommended concerning this affinity constant.

At this stage of the discussion, we may conclude that the model was able to predict both inhibition and toxic effects on the nitrifying sludge activity; however the unavailability of direct measurements of cell physiological damage due to the presence of benzene does not allow more realistic conclusions. Finally, the present model may be easily extended to study cases where growth and decay may be neglected as it was assumed in this work.

#### 4.2. Parameter sensitivity analysis

The parameter sensitivity analysis indicates which kinetic parameters most affected the ability of the model to predict ammonia oxidation, nitrite oxidation and benzene transformation. Model ability to fit ammonia, nitrite, nitrate and benzene concentrations using the experiment with  $S_{\text{BZ}}(0) = 10 \text{ mg benzene-C l}^{-1}$  was investigated by changing values of the estimated model parameters. Minimum and maximum levels of the kinetic parameters of the nitrification model were established by considering value changes  $\Delta P = -10\%$  and  $\Delta P = +10\%$ , respectively. Simulations were carried out by varying one parameter at a time, as the remaining parameters were held constant at their nominal values (Table 1). Sensitivity was assessed by computing the mean of the absolute errors between the simulation with the nominal value and with one modified parameter, for ammonia, nitrite, nitrate and benzene concentrations. These absolute errors were calculated for each of the 24-h simulation period, and then the mean was obtained. As shown in Table 3, perturbations on the ammonium oxidation related parameters are influencing the ammonia, nitrite and nitrate model predictions while the nitrite oxidation related parameters are only affecting nitrite and nitrate, which is explained by the two-step structure of the model. The kinetic parameter having the most notable impact

**Table 3**  
Results of the parameter sensitivity analysis (MAE = mean absolute error,  $\Delta P = -10\%$  (left),  $\Delta P = +10\%$  (right)).

Parameter	Nominal value	MAE $S_{NH_4}$ (mg N l <sup>-1</sup> )	MAE $S_{NO_2}$ (mg N l <sup>-1</sup> )	MAE $S_{NO_3}$ (mg N l <sup>-1</sup> )	MAE $S_{BZ}$ (mg C l <sup>-1</sup> )
$Y_{PA}$	0.91	0.00/0.00	0.82/1.13	3.68/3.37	0.00/0.00
$K_{S,A}$	1.8	0.15/0.15	0.04/0.04	0.10/0.10	0.00/0.00
$K_{i,A}$	23.8	1.16/0.98	0.21/0.20	0.90/0.75	0.00/0.00
$K_{t,A}$	0.95	1.73/1.62	0.32/0.36	1.3001.21	0.00/0.00
$\delta_A$	0.11	2.46/2.30	0.44/0.54	1.86/1.71	0.00/0.00
$Y_{PN}$	1	0.00/0.00	0.00/0.00	4.15/4.15	0.00/0.00
$K_{S,N}$	1.9	0.00/0.00	0.32/0.32	0.32/0.32	0.00/0.00
$K_{i,N}$	36.2	0.00/0.00	0.16/0.12	0.16/0.12	0.00/0.00
$K_{t,N}$	9.5	0.00/0.00	2.54/1.07	2.53/1.06	0.00/0.00
$\delta_N$	0.12	0.00/0.00	0.12/0.12	0.12/0.12	0.00/0.00
$K_{S,BZ}$	1.85	0.04/0.04	0.01/0.01	0.04/0.04	0.06/0.05
$K_{i,BZ}$	46.1	0.24/0.22	0.03/0.03	0.22/0.20	0.25/0.21

on the ammonium concentration is clearly the toxicity parameter  $\delta_A$ . This occurrence stigmatizes the fact that this particular parameter has to be determined very accurately in order to generate good model predictions, which is fortunately the case here since its estimated relative standard deviation (Table 1) is equal to 14%.  $Y_{PN}$  is the most sensible parameter but it affects exclusively the nitrate concentration predictions and also has a relatively good standard deviation. We may as well notice that the model is showing an important sensitivity to the benzene inhibition constants ( $K_{i,A}$ ,  $K_{i,N}$ ) and toxicity constants ( $K_{t,A}$ ,  $K_{t,N}$ ), confirming the importance of integrating the related mechanisms in the nitrification model. Finally, if it is desired to express the process kinetic in terms of specific rather than volumetric oxidation rates, accurate estimation or experimental measurement of ammonium-oxidizing biomass  $X_A$  and nitrite-oxidizing biomass  $X_N$  initial concentrations becomes necessary to avoid well known identifiability issues.

## 5. Conclusions

A two-step nitrification model that explicitly takes into account both inhibitory and toxic effects of benzene present in batch nitrifying cultures was derived in this study. Experimental data and model predictions presented an adequate fitting for different batch cultures corresponding to different initial concentrations of benzene. In particular, the model was able to predict the fact that both ammonia and nitrite-oxidizing activity were affected by benzene presence. Moreover, additional toxicity batch tests allowed the integration of the benzene toxic effect through the modulation of the maximum volumetric oxidation rate of ammonium and nitrite as a function of the initial benzene concentration of the preexposed culture. Standard deviations, correlation between parameters and a sensitivity analysis of the estimated parameters were also provided. Therefore, this dynamical model may be used as a prediction tool in the design of control strategies for improving the biological treatment of nitrifying wastewaters in presence of BTEX.

## Acknowledgments

This research was supported by PROMEP (103.5/07/2554) and CONACYT (400200-5-33668-U.160302 and 61787).

## References

- [1] K. Chandran, B.F. Smets, Single-step nitrification models erroneously describe batch ammonia oxidation profiles when nitrite oxidation becomes rate limiting, *Biotechnol. Bioeng.* 68 (2000) 396–406.
- [2] I. Iacopozzi, V. Innocenti, S. Marsili-Libelli, E. Giusti, A modified Activated Sludge Model No. 3 (ASM3) with two-step nitrification–denitrification, *Environ. Model. Softw.* 22 (2007) 847–861.
- [3] N. Checchi, S. Marsili-Libelli, Reliability of parameter estimation in respirometric models, *Water Res.* 39 (2005) 3686–3696.
- [4] G. Baquerizo, J.P. Maestre, T. Sakuma, M.A. Deshusses, X. Gamisans, D. Gabriel, J. Lafuente, A detailed model of a biofilter for ammonia removal: model parameters analysis and model validation, *Chem. Eng. J.* 113 (2005) 205–214.
- [5] K. Chandran, B.F. Smets, Applicability of two-step models in estimating nitrification kinetics from batch respirograms under different relative dynamics of ammonia and nitrite oxidation, *Biotechnol. Bioeng.* 70 (2000) 54–64.
- [6] S. Marsili-Libelli, P. Ratini, A. Spagni, G. Bortone, Implementation, study and calibration of a modified ASM2d for the simulation of SBR processes, *Water Sci. Technol.* 43 (2001) 69–76.
- [7] A.C. Texier, J. Gomez, Tolerance of nitrifying sludge to *p*-cresol, *Biotechnol. Lett.* 24 (2002) 321–324.
- [8] U.S. Environmental Protection Agency, National primary drinking water regulations, *Fed. Reg.* 19 (2001) 141.
- [9] S.W. Chang, H.J. La, S.J. Lee, Microbial degradation of benzene, toluene, ethylbenzene and xylene isomers (BTEX) contaminated groundwater in Korea, *Water Sci. Technol.* 44 (2001) 165–171.
- [10] L.D. Collins, A.J. Daugulis, Simultaneous biodegradation of benzene, toluene, and *p*-xylene in a two-phase partitioning bioreactor: concept demonstration and practical application, *Biotechnol. Prog.* 15 (1999) 74–80.
- [11] A. Zepeda, A.C. Texier, J. Gomez, Batch nitrifying cultures in presence of mixture of benzene, toluene and *m*-xylene, *Environ. Technol.* 28 (2007) 355–360.
- [12] A. Zepeda, A.C. Texier, E. Razo, J. Gomez, Kinetic and metabolic study of benzene, toluene, and *m*-xylene in nitrifying batch cultures, *Water Res.* 40 (2006) 1643–1649.
- [13] A. Zepeda, A.C. Texier, J. Gomez, Benzene transformation in nitrifying batch cultures, *Biotechnol. Prog.* 19 (2003) 789–793.
- [14] T. Vannelli, A.B. Hooper, NIH shift in the hydroxylation of aromatic compounds by the ammonia-oxidizing bacterium *Nitrosomonas europaea*. Evidence against an arene oxide intermediate, *Biochemistry* 34 (1995) 11743–11749.
- [15] W.K. Keener, D.J. Arp, Transformations of aromatic compounds by *Nitrosomonas europaea*, *Appl. Environ. Microbiol.* 60 (1994) 1914–1920.
- [16] M.R. Hyman, A.W. Sansone-Smith, J.H. Shears, P.M. Wood, A kinetic study of benzene oxidation to phenol by whole cells of *Nitrosomonas europaea* and evidence for the further oxidation of phenol to hydroquinone, *Arch. Microbiol.* 143 (1985) 302–306.
- [17] T. Yano, S. Koga, Dynamic behavior of the chemostat subject to substrate inhibition, *Biotechnol. Bioeng.* 11 (1969) 139–153.
- [18] S. Isken, P.M.A.C. Santos, J.A.M. de Bont, Effect of solvent adaptation on the antibiotic resistance of *Pseudomonas putida* S12, *Appl. Microbiol. Biotechnol.* 48 (1997) 642–647.
- [19] S. Isken, J.A.M. de Bont, Bacteria tolerant to organic solvents, *Extremophiles* 2 (1998) 229–238.
- [20] J. Sikkema, J.A.M. de Bont, B. Poolman, Interactions of cyclic hydrocarbons with biological membranes, *J. Biol. Chem.* 11 (1994) 8022–8028.
- [21] J. Sikkema, J.A.M. de Bont, B. Poolman, Mechanisms of membrane toxicity of hydrocarbons, *Microbiol. Rev.* 59 (1995) 201–222.
- [22] I.V. Tsitko, G.M. Zaitsev, A.G. Lobanok, M.S. Salkinoja-Solonen, Effect of aromatic compounds on cellular fatty acid composition of *Rhodococcus opacus*, *Appl. Environ. Microbiol.* 65 (1999) 853–855.
- [23] H.J. Heipieper, B. Löffel, H. Keweloh, J.A.M. de Bont, The Cis/Trans isomerisation of unsaturated fatty acids in *Pseudomonas putida* S12: an indicator for environmental stress due to organic compounds, *Chemosphere* 30 (1995) 1041–1051.
- [24] D. Dochain, P.A. Vanrolleghem, M. Van Daele, Structural identifiability of biokinetic models of activated sludge respiration, *Water Res.* 29 (1995) 2571–2578.
- [25] P.A. Vanrolleghem, D. Dochain, Bioprocess model identification, in: J.F.M. Van Impe, P.A. Vanrolleghem, D. Iserentant (Eds.), *Advanced Instrumentation, Data Interpretation and Control of Biotechnological Processes*, Kluwer, Dordrecht, 1998, pp. 251–318.
- [26] L. Ljung, *System Identification—Theory for the User*, Prentice Hall, Englewood Cliffs, New Jersey, 1987.
- [27] K.R. Godfrey, J.J. Di Stephano, Identifiability of model parameters, in: *Identification and System Parameter Estimation*, Pergamon Press, Oxford, 1985, pp. 89–114.
- [28] W. Squire, G. Trapp, Using complex variables to estimate derivatives of real functions, *SIAM Rev.* 40 (1998) 110–112.
- [29] D.J.W. De Pauw, Optimal experimental design for calibration of bioprocess models: a validated software toolbox, Ph.D. Thesis, BIOMATH, University of Gent, 2005.